A Charge-Pump Passive-Matrix Pixel Driver for Organic Light Emitting Diodes

Jong-Wook Seo, Hanbyul Kim, Bongok Kim, and Youngkwan Kim
Dept. of Electronics Engr. and Dept. of Chemical Engr., Hongik University,
Sangsu-dong, Mapo-gu, Seoul 121-791, Korea
Phone : +82-2-320-1663, E-mail : jwseo@wow.hongik.ac.kr

Abstract

A new pixel driving method for organic light-emitting diode (OLED) flat-panel display (FPD) is proposed. The new charge-pump passive-matrix pixel driver consists only of a storage capacitance and a rectifying diode, and no thin-film transistor (TFT) is needed. The new driver not only supplies a constant current to the OLED throughout the whole period of panel scanning like an active-matrix driver, but also provides a highly linear gray-scale control through a pure digital manner.

1. Introduction

Although the self-emissive OLED has various advantages such as light-weight, potential of low-cost processes, and low power consumption compared to the other existing display technologies, its advance into the market has been impeded by the lack of proper pixel driving methods. Passive-matrix (PM) and active-matrix (AM) pixel driving methods are common approaches in the OLED FPD area [1], [2]. A conventional PM pixel driver activates an OLED cell for only a short period of time by applying a short pulse of either electric current or voltage. As the address line time becomes so short for the modern high information content display, electric current pulses with disturbingly large amplitudes are required to get a high enough luminance [3]. Therefore, it becomes less feasible for the PM drivers to be used in wide panel OLED FPD due to the performance and reliability issues in spite of its simple structure and ease of fabrication. The long-term reliability, efficiency, and performance of the conventional PM-OLED display are then jeopardized by the high-current shock, particularly, due to heat generation.

On the other hand, an AM driver activates an OLED cell during the whole period of panel scanning by current driving circuitry using TFT's. However, the TFT-based AM-OLED has made little progress in its application to commercial products. Unlike an AM-LCD, an AM-OLED requires not only a multiple number of TFT's, but also finely controlled device parameters and operation conditions because its operation is so sensitive to the device parameters [4]. Additionally, the multiple-TFT driver is accompanied by an increased number of interconnections thus by the increased circuit and process complexity [5]. It is also extremely hard to achieve an accurate gray-level control for the TFT-based AM-OLED display [6]-[8]. Consequently, it has become the prime concern to develop a new easy-to-fabricate pixel driving circuit that delivers a continuous current signal to an OLED and that provides an accurate gray-scale control as well. In this work, a new TFT-free passive-matrix pixel driving method using a charge-pump scheme is proposed. The new method utilizes the characteristic properties – high response speed and current-based operation – of the OLED devices. The operation principle, design, and experimental results are presented.

2. Operation Principle

Figure 1 shows the schematic of the 2-dimensional cell array with the charge-pump pixel drivers for an OLED display panel. As can be seen from the figure, a charge-pump consists of a rectifying diode depicted by D and a storage capacitance depicted by C. The basic operation of the driver is a consecutive charging and discharging of the storage capacitance through the rectifying diode and the OLED, respectively. The operation is achieved by driving each row of the pixel matrix using a row-drive signal $R_i(t)$ for row i, and the typical waveform is shown in Fig. 2(a). A complete cycle of the row-drive signal is composed of *charging time* ($0 \le t \le t_{charge}$) and *discharging time* ($t_{charge} \le t \le t_{scan}$) as shown in the figure. The period of the row-drive signal is determined by the video frame rate and the number of gray levels to achieve, and the phases

of the signals for the adjacent rows are $2\pi/M$ different from each other as shown in Fig. 2(b).

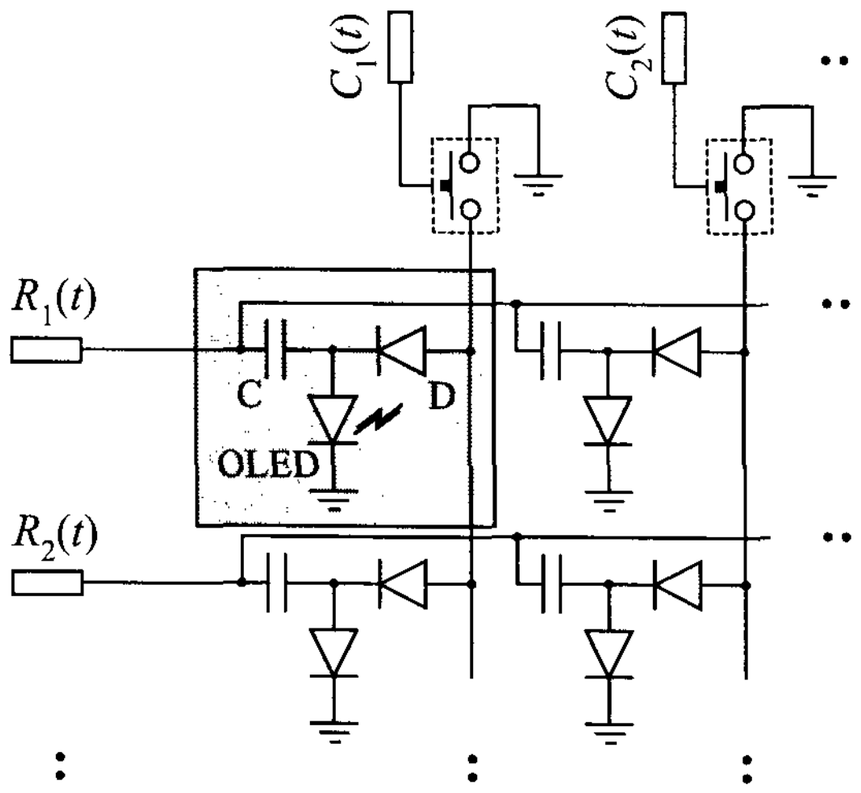

Figure 1 Schematic of the array of charge-pump pixel drivers.

The light emission from the OLED cells can be turned on and off as the column switches shown at the top of Fig. 1 are turned on and off, respectively, by the column-drive signals of which a typical waveform is shown in Fig. 2(c). As the row-drive signals pull down the row voltages at their charging times in sequence, the column-drive signals turn on or off the switches depending on the video data for the corresponding cells. The cell whose switch is turned on at its charging time will emit light during the full panel-scan period as represented in Fig. 2(d). On the other hand, the cell turned off will remain dark.

The amplitude and shape of the current through an OLED cell is determined mainly by the row-drive signal particularly by the peak voltage at the end of charging time and the waveform during the discharging time, and the average current can be estimated by considering the alteration of the charge stored in the storage capacitance. First consider the case that the column switch is turned on during the charging time. Electric current flows through the rectifying diode to charge the capacitance during the charging time, and the amount of the charge Q_{charge} stored in the storage capacitance at the end of the charging time is determined by the voltage across it:

$$Q_{\text{charge}} = C_s V_{\text{C,charge}} = -C_s \left[V_{\text{R(t),charge}} + V_D \right] \quad (1)$$

where C_s is the storage capacitance, $V_{\text{C,charge}}$ is the capacitance voltage with respect to the row drive line whose voltage is $V_{\text{R(t),charge}}$, and V_D is the voltage drop at the rectifying diode. The voltage drop at the column switch is ignored, and the RC time constant of the charging path is assumed to be short enough compared to the charging time when the diode is ON state. Meanwhile, the stored charge at the end of the discharging time is given by

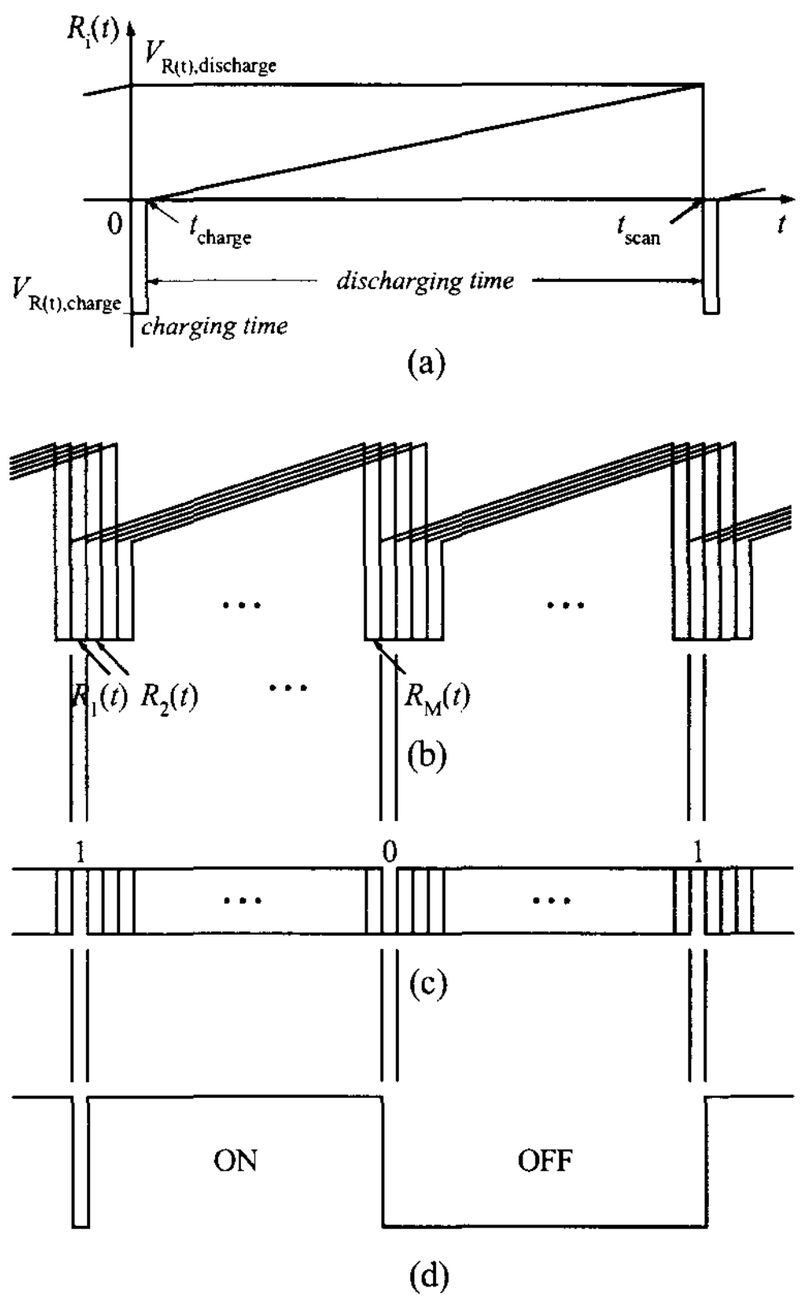

Figure 2 (a) The typical waveform of the row-drive signal $R_i(t)$. (b) The phase relationship between the row-drive signals for some adjacent rows. (c) The typical waveforms of the column-drive signal $C_j(t)$. (d) A typical OLED current waveform corresponding to the column-drive signal shown in (c).

$$Q_{\text{discharge}} = C_s V_{\text{C,discharge}} = -C_s \left[V_{\text{R(t),discharge}} - V_{\text{OLED}} \right] \quad (2)$$

where $V_{\text{C,discharge}}$ is the capacitance voltage with respect to the row-line voltage $V_{\text{R(t),discharge}}$, and V_{OLED} is the

voltage drop at the OLED. Then, the average OLED current I_{OLED} during the discharging time is given by the temporal variation of the electric charge stored in the capacitance:

$$I_{OLED} = \frac{Q_{charge} - Q_{discharge}}{t_{scan} - t_{charge}} = \frac{C_s}{t_{scan} - t_{charge}}\left[\Delta V_{R(t),pp} - \left(V_D + V_{OLED}\right)\right] \quad (3)$$

where t_{scan} and t_{charge} are the row-scan period and the duration of the charging time, respectively, and $\Delta V_{R(t),pp}$ is the peak-to-peak voltage of the row-drive signal.

Equation (3) gives the rule of thumb to design the storage capacitance and the waveform of the row-drive signal. It can be seen from the equation that having short t_{scan} and t_{charge} is favorable to make C_s small and $\Delta V_{R(t),pp}$ low. It means that no conflict exists between the design of an easier-to-fabricate charge-pump driver and the getting of a finer gray-scale and/or more pixel lines for higher information content, apparently, within the limit of the system *RC*-delay. It is also favorable to have a 1st-order dependence between the voltages and the OLED current unlike in a TFT-based active-matrix driver that has the well known 2nd-order dependence of a field-effect transistor causing higher device sensitivity. Additionally, the sensitivity of I_{OLED} to V_{OLED} can be made even smaller by making the voltage much smaller than $\Delta V_{R(t),pp}$.

Meanwhile, in case that the column switch is turned off during the charging time, no current flows through the OLED because no external charge is driven into the storage capacitance during the charging time. The capacitance charge is from the junction capacitances of the rectifying diode and the OLED, and it returns to the junctions again during the discharging time instead of being injected into the active EL layer to produce photons. Additionally, it is obvious that the above-mentioned charge flow path – rectifying diode and then OLED - is the only possible one ensuring a crosstalk-free operation.

3. Experiments and Discussions

Figure 3(a) shows the red-color OLED with an area of 2.5 × 2.5 mm^2 used in the study. The one in the left of the figure is that in the ON state and the other one in the right is that in the OFF state. Figure 3(b) shows the measured *I-V* characteristics of the device. The inset of Fig. 3(b) is the same relationship with the current in log scale. The pixel driver circuit for the test cell was built using a 1N4148 silicon *pn*-junction diode and a 12 nF capacitance. Since the capacitance value determines the total current thus the brightness of the OLED, it should be determined based on the aimed luminance of the OLED. The capacitance value was chosen to get a luminance of 100 cd/m^2, which is known to be that required for commercial applications, and the luminance was measured to be 110 cd/m^2. The large capacitance value in the test circuit is the result of the extraordinarily large area of the test cell. A capacitance of approximately 10 pF will be needed for a 100 × 100 μm^2 wide OLED cell to get an 8-bit gray scale and a luminance of 100 cd/m^2. The row-drive signal was generated by a universal function generator, and a *Hitachi* J182 silicon PMOS transistor was used as the column switch, which is controlled by the logic circuits built by TTL gates.

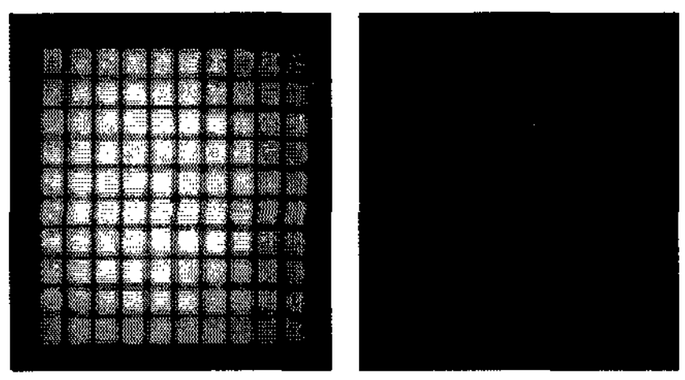

(a)

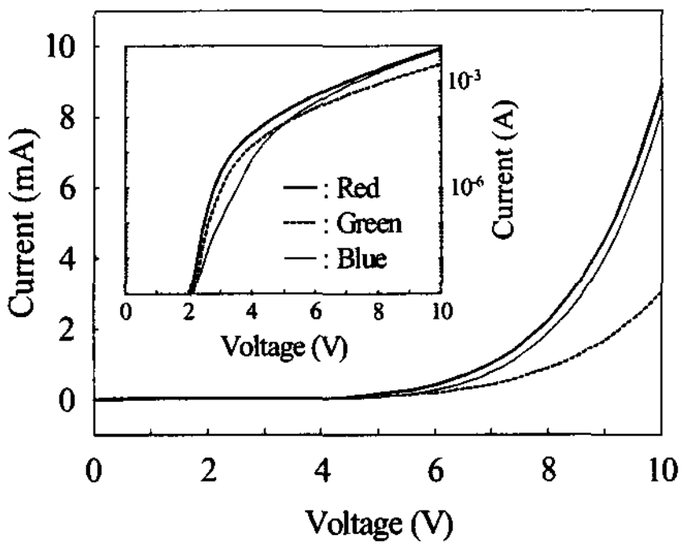

(b)

Figure 3 (a) Photographs of the OLED in ON (left) and OFF (right) states. (The speckles on the surface of the OLED under OFF state are due to the light reflection.) (b) The typical *I-V* characteristics of the OLED's.

Figure 4 shows the typical waveforms of the row-

drive signal applied to the OLED and the resulting light output from the cell. The row-drive signal shown in Fig. 4(a) is the one that corresponds to a 30 fps frame rate, 8-bit (256) gray scale, and 100 row lines to scan. The signal period and the charging time are t_{scan} = 130 μsec (= 1 / (30 frame/sec × 256 scans/frame)) and t_{charge} = 1.3 μsec (= t_{scan} / 100 lines), respectively. The light output was measured using an *Acton Research Corporation* PD-438 photomultiplier tube (PMT) with a bias voltage of 300 V and a load resistance of 50 Ω. As can be seen from Fig. 4(b), the light output from the OLED lasts for the whole period of the drive signal as in an AMOLED except during the short charging time. The slow turn-on of the light at the leading edge of the discharging time is believed to be due to the large capacitance, which was measured to be 0.7 nF, of the OLED cell.

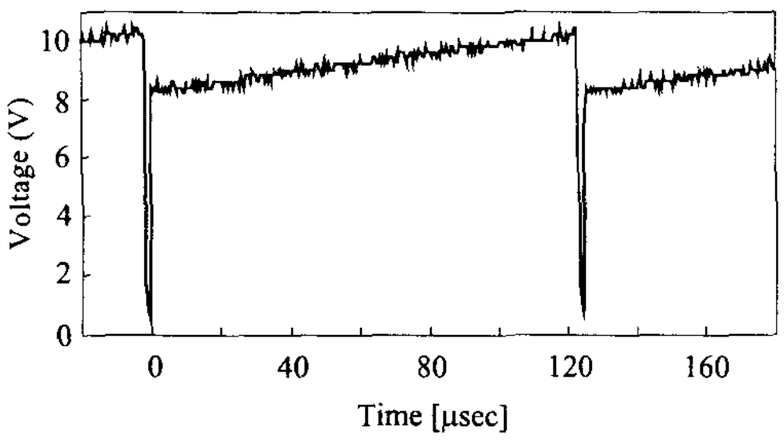

Figure 4 (a) The row-drive signal corresponding to 30 fps frame rate, 8-bit (256) gray scale, and 100 lines to scan, and (b) the corresponding light emission pattern from the OLED.

Figure 5 shows some typical examples of the variation of the light emission pattern for various row-drive signal waveforms. As can be seen from the figure, the light emission from the cell is strongly dependent on the row-drive signal waveform, particularly on its start-up voltage at the beginning of the discharging time. As the drive signal starts at a higher voltage, the light emission at the forefront of the discharging time becomes dominant and vice versa. Apparently, there exists an optimal voltage waveform for the row-drive signal to get a maximally flat light output. Nevertheless, the light emission is elongated in time significantly, and it is achieved by the process of keeping electrical charges in the storage capacitance and then subsequently pumping them into the OLED. The total light intensity emitted from the OLED cell varies by only a small factor even if a row-drive signal with a simple pulse shape was used. It is a big difference from the conventional PM-OLED where light emission is highly concentrated within the line time.

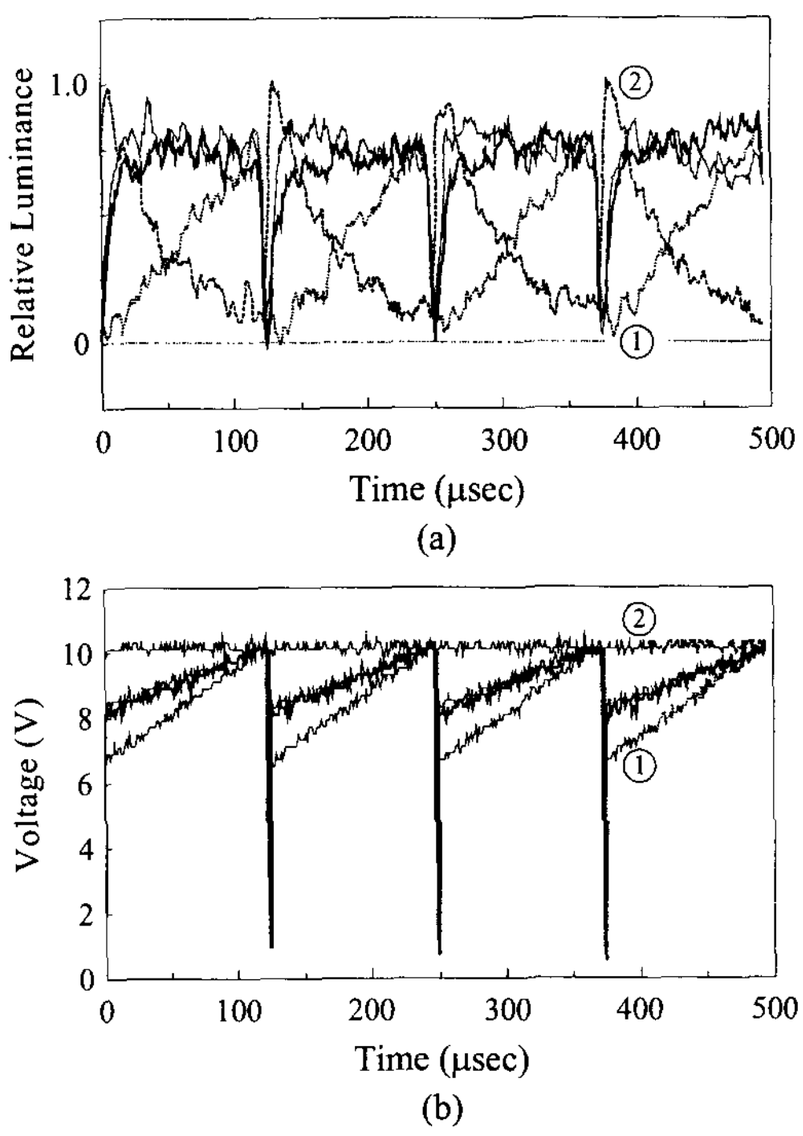

Figure 5 (a) The variation of light emission pattern corresponding to (b) the variation of the row-drive signal waveform.

The operation speed of the OLED is so fast that it responds to the driving current almost instantaneously up to the megahertz range of operation. Therefore, it is possible to control the gray scale of a pixel in a pure digital manner simply by controlling the total number of charge-pumping into the OLED cell during a frame period as depicted in Fig. 6(a). The figure shows the case of an 8-bit gray scale (256 gray levels) where a pixel will be scanned 255 times during a frame period. A pixel is pumped with electric charge for only a certain number of scans depending on the attempted

gray level. The darkest level is that corresponding to an all-time OFF operation, whereas the brightest level is that corresponding to an all-time ON operation. An intermediate gray level is in between proportional to the gray level.

Figure 6(b) shows the variation of the gray level as the number of turn-on counts is increased from 0 to 255 for linear gray-scale control. The luminance was measured using the *Advantest* TQ8210 optical power meter with TQ82014 power sensor, and the dark current component from the power meter was subtracted from the measured light intensity values. As can be seen from the figure, an almost linear gray-level control has been achieved. No light was emitted from the pixel when the turn-on count was set to be 0 for the darkest gray level, and this is very much favorable to obtain a high contrast ratio. The high degree of linearity implies that the operation speed of the OLED cell is fast enough to be free from any inter-symbol interference. Since light emission from the OLED stops immediately at the end of the row-drive signal as can be seen from Fig. 4(b), the total luminance is independent of the number of turn-on counts. This is another distinguishing feature of the charge-pump pixel driver from the TFT-based one [9].

4. Conclusions

A new method of pixel driving for OLED FPD is proposed. The new pixel driver supplies a constant current to the OLED cell throughout the whole period of panel scanning like an active-matrix driver, and an improvement in long-time reliability and power efficiency of the device can be achieved. The new pixel driver consists only of a storage capacitance and a rectifying diode. Since no TFT is required for the new circuit, the manufacturing processes can be made simple. It is also possible to control the gray level in a pure digital format to provide a highly linear gray scale. Additionally, the new TFT-free approach can minimize the dependence of the circuit operation on the manufacturing variation and aging of device characteristics and operation conditions. It is also shown that the new method can provide a pure digital way of gray-level control to achieve a very precise gray scale.

Acknowledgements

The authors would like to thank Samsung NEC Mobile Display Co., Ltd. in Korea for the OLED samples used in the study. This work is partially supported by ITRC-CHOAN and Korea Science and Engineering Foundation (No. R01-2000-00258).

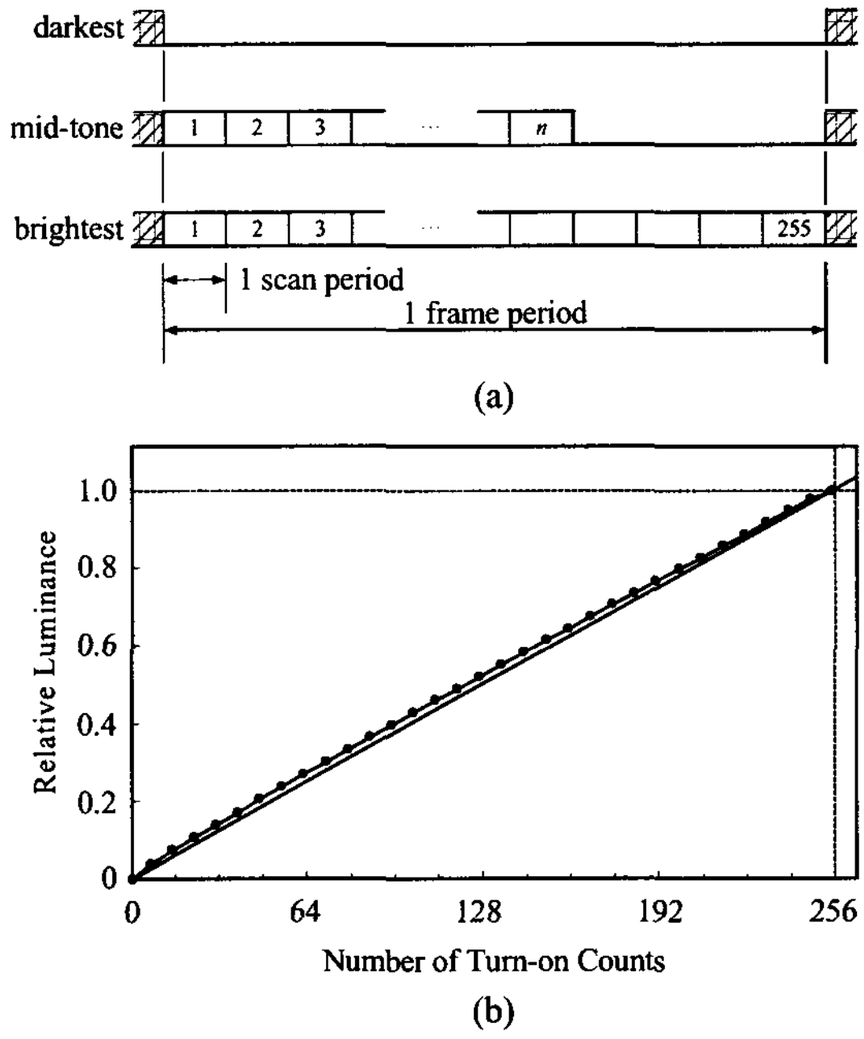

Figure 6 (a) The schematic representation of the column-drive patterns for some attempted gray levels. (b) Measured cell luminance vs. the number of turn-on counts.

5. References

[1] D. Pribat and F. Plais, Thin Solid Films, 383, 25 (2001).

[2] G.. Gu and S. R. Forrest, IEEE J. Selected Topics in Quantum Electron., 4, 83 (1998).

[3] S. Xiong, B. Guo, C. Wu, Y. Chen, Y. Hao, Z. Zhou and H. Yang, SID02DIGEST, 1174 (2002).

[4] R.M.A. Dawson, *et al.*, SID98DIGEST, 11 (1998).

[5] M. Stewart, R. S. Howell, L. Pires, and M. K. Hatalis, W. Howard and O. Prache, Tech. Dig. IEDM, 871 (1998).

[6] R. Hattori, T. Tsukamizu, R. Tsuchiya, K. Miyake, Y. He and J. Kanicki, IEICE Trans. Electron., E83-C, 779 (2000).

[7] Y. He, R. Hattori and J. Kanicki, Jpn. J. Appl. Phys., 40, 1199 (2001).

[8] V. Bulovic, P. E. Burrows and S. R. Forrest, Semiconductors and Semimetals, 64, 255 (2000).

[9] R. M. A. Dawson, *et al*, Tech. Dig. IEDM, 875 (1998).